

TMU-NT931001
October 1993

Diquark Correlations in the Nucleon Structure Function

Katsuhiro Suzuki, Takayuki Shigetani and Hiroshi Toki*

Department of Physics, Tokyo Metropolitan University

Hachiohji, Tokyo 192, Japan

Abstract : The nucleon structure functions are studied with a special emphasis on diquark correlations inside the nucleon. Assuming a phenomenological diquark-quark model of the nucleon at the low energy hadronic scale, we calculate the leading twist contributions to the nucleon structure functions. We take the Nambu and Jona-Lasinio model for the calculation of the quark distributions in the diquarks, and use the convolution method for the diquark scattering process. The resulting quark distributions are evolved to the experimental momentum scale using the perturbative QCD. We discuss the flavor dependence of the nucleon structure functions and the importance of the quark-quark correlations for the understanding of the nucleon structure.

*also RIKEN, Wako, Saitama, 351, Japan

1 Introduction

Recent measurements of deep inelastic scattering show clear flavor dependences of the nucleon structure functions[1-3]. One example is the ratio of the neutron to proton structure functions $F_2^n(x)/F_2^p(x)$ which shows a large deviation from the naive quark-parton model prediction, which is 2/3. In addition, the recent NMC data shows that the difference between the Q^2 dependence of $F_2^p(x)$ and $F_2^n(x)$ is substantially larger than the perturbative QCD prediction[2].

On the other hand, the diquark-quark model of the nucleon has attracted considerable interests. The idea of diquarks, i.e. correlated states of two quarks, is introduced phenomenologically to explain the scaling violation of the nucleon structure functions, which may be caused by the non-perturbative diquark correlations[4]. The diquark model also reproduces the proton-neutron differences of the structure functions[5]. Such a diquark structure is due to the quark-quark correlations which depend on its flavor structure, and may produce an asymmetry of the momentum distribution in the nucleon. In fact, such asymmetric momentum distributions are found in the calculations of the QCD sum rule[6, 7], where the most part of the proton momentum is carried by the u-quark with its spin directed along the proton spin and the remaining small part is carried by the u-d quarks with combined spin-0. Additionally, the elastic form factor of the nucleon requires an asymmetric momentum distributions, which indicates the diquark clustering inside the nucleon[8]. This model is also supported by the study of several high energy scattering processes[9, 10].

In the low energy side of the hadron physics, the diquark-quark structure of baryons also plays various roles[10, 11, 12]. This picture was first introduced to explain the universality of the Regge trajectories[11]. In particular, a recent work of Stech and his collaborators showed that the diquark correlations, which are the strongest in the scalar diquark channel, can account for the $\Delta I = 1/2$ problem of weak non-leptonic transitions, and reproduce the experimental data very well[13, 14]. Hence, it is of our great interest to study the flavor dependence of the nucleon structure in terms of the diquark-quark model as a successful low energy model of baryons. We note that such an approach naturally reproduces the

asymmetry of momentum distributions in the nucleon obtained by the QCD sum rule.

Several theoretical calculations of the nucleon structure function were made in terms of the low energy quark models[15-20]. The structure function at the low energy scale $Q^2 = Q_o^2$, where the phenomenological quark model is supposed to work, is obtained by calculating the twist-2 matrix elements, since these matrix elements are dominant over higher twist terms in the Bjorken limit. The resulting structure functions are evolved to the experimental scale with the help of the perturbative QCD. Thus, one can compare them with experimental data. Here, we use the same method to evaluate quark distributions within the diquark model.

Recently, the importance of the quark-diquark intermediate state in the calculation of the nucleon structure function was discussed within the MIT bag model[19] and the quark-diquark model[20]. It was pointed out that the mass difference between the scalar(0^+) and the axial-vector(1^+) diquarks is crucial to account for the flavor dependence of quark distributions, since this mass difference produces the dominance of u-quark distribution in the proton at large Bjorken x . In such works, the diquarks are treated only as a spectator. However, if the two quark correlation is so strong as obtained in the QCD sum rule, we should take into account the diquark scattering process explicitly with the other quark being a spectator.

In this paper, we shall calculate the nucleon structure function in the framework of the $SU(6)$ diquark-quark model. Thus, both quark and diquark scattering processes contribute to the structure function, which are illustrated in Fig.1(a) and (b). The process of Fig.1(a), in which a quark is struck out by the virtual photon with the residual diquark being a spectator, is evaluated by using the standard method in the impulse approximation[20]. For the diquark part, we use the convolution technique[21, 22] to calculate contributions of the diquark process shown in Fig.1(b). We obtain the diquark terms as the convolution of quark distributions in diquarks with the diquark distributions in the nucleon. This diagram represents the leading twist contributions of diquarks, in which diquarks break up completely after absorbing the virtual photon[4]. Hence, the resulting quark distributions scale; i.e.

there is no Q^2 dependence without the QCD radiative correction. Here, we shall not calculate the twist-4 non-scaling contributions of diquarks, which are under consideration[23].

2. Nucleon Structure Function in the Diquark model

The $SU(6)$ diquark-quark wave function of proton is written as[12],

$$|p \uparrow\rangle = \frac{1}{\sqrt{18}} [3S(ud)u \uparrow + 2A(uu)^+d \downarrow - \sqrt{2}A(uu)^o d \uparrow - \sqrt{2}A(ud)^+u \downarrow + A(ud)^o u \uparrow] \quad (1)$$

where $S(ij)$ denotes the scalar (spin singlet; 0^+) diquark with the flavor content i and j , and $A(ij)^\kappa$ the axial-vector (spin triplet; 1^+) diquark with the helicity κ . In this model, both the quark and the diquark scattering processes contribute to the hadronic tensor. Using (1), the proton and the neutron structure functions are given by,

$$F_2^p(x) = \frac{2}{9}q^S(x) + \frac{1}{9}q^V(x) + \frac{5}{18}Q_D^S(x) + \frac{7}{18}Q_D^V(x) \quad (2-a)$$

$$F_2^n(x) = \frac{1}{18}q^S(x) + \frac{1}{6}q^V(x) + \frac{5}{18}Q_D^S(x) + \frac{1}{6}Q_D^V(x) \quad (2-b)$$

where q^S and q^V are the quark distributions with the residual diquarks being the scalar and the axial-vector diquarks, respectively. Q_D^S and Q_D^V are the quark distributions obtained by the scalar and the axial-vector diquark scattering processes, respectively. We can also express the valence distributions of the u and d quarks in the proton as,

$$u(x) = \frac{1}{2}q^S(x) + \frac{1}{6}q^V(x) + \frac{1}{2}Q_D^S(x) + \frac{5}{6}Q_D^V(x) \quad (3-a)$$

$$d(x) = \frac{1}{3}q^V(x) + \frac{1}{2}Q_D^S(x) + \frac{1}{6}Q_D^V(x) \quad (3-b)$$

Note that $q^S(x)$ term contributes only to the u-quark distribution. The flavor dependence of the structure functions arises from the difference of the distribution contents in this model. We also note that the definition (2-a,2-b), (3-a,3-b) is different from that of the previous work[5, 24], in which the diquarks are assumed to be point-like. We consider the scaling contributions of diquark processes, where the diquarks are broken up completely by the virtual photon.

3 Nambu and Jona-Lasinio model

We use the Nambu and Jona-Lasinio (NJL) model to take into account the quark correlations, where the chiral invariance is the main ingredient[25]. Recently, the NJL model is studied in various subjects of hadron physics as a low energy effective theory of QCD[26]. This model describes the $SU(3)_f$ meson properties very well with the parameters fixed by the pion and the kaon properties, in spite of the lack of confinement. The $SU(3)$ NJL lagrangian for mesons is given by[26],

$$\begin{aligned}
 \mathcal{L}_{NJL} &= \mathcal{L}_o + \mathcal{L}_M \\
 \mathcal{L}_o &= \bar{\psi}(i\gamma^\mu\partial_\mu - m_o)\psi \\
 \mathcal{L}_M &= G_S^M[(\bar{\psi}t_a\psi)^2 + (\bar{\psi}t_a i\gamma^5\psi)^2] \\
 &\quad - G_V^M[(\bar{\psi}t_a\gamma_\mu\psi)^2 + (\bar{\psi}t_a\gamma_\mu\gamma^5\psi)^2]
 \end{aligned} \tag{4}$$

Here ψ denotes quark fields and m_0 their bare masses. t_a are the flavor $SU(3)_f$ operators with the normalization $tr(t_a t_b) = \delta_{ab}/2$, and G_S^M , G_V^M are the coupling constants. In this model, the quarks acquire the constituent masses dynamically due to the spontaneous breakdown of the chiral symmetry. The meson masses are obtained by solving the Bethe-Salpeter (BS) equation.

On the other hand, the NJL lagrangian for the quark-quark interaction at the Fierz

transformed level is given by[26,27],

$$\begin{aligned}
\mathcal{L}_D = & G_S^D [(\bar{\psi} t_a c_A \psi_c)(\bar{\psi}_c t_a c_A \psi) + (\bar{\psi} t_a c_A i\gamma^5 \psi_c)(\bar{\psi}_c t_a c_A i\gamma^5 \psi)] \\
& - G_V^D [(\bar{\psi} t_s c_A \gamma^\mu \psi_c)(\bar{\psi}_c t_s c_A \gamma_\mu \psi) \\
& + (\bar{\psi} t_a c_A \gamma^\mu \gamma^5 \psi_c)(\bar{\psi}_c t_a c_A \gamma_\mu \gamma^5 \psi)]
\end{aligned} \tag{5}$$

Here, $\psi_c = C\bar{\psi}^T$ are the charge conjugate quark fields and c_A the antitriplet color $SU(3)$ operators with the normalization $tr(c_i c_j) = \delta_{ij}/2$, where A runs over only $A = 2, 5$ and 7 . The flavor suffix a runs over $a = 2, 5$ and 7 for pseudoscalar, scalar and vector diquark terms, while it runs over $s = 0, 1, 3, 4, 6$ and 8 for the axial-vector diquark term due to the antisymmetrization of diquarks. Note that the presence of the charge conjugation operator produce an additional minus sign to the parity of diquarks. We get the masses and the wave functions of diquarks by solving the quark-quark BS equations as the case for mesons. Recently, the diquark structure is extensively studied in the framework of the NJL model[26]. We find that the structure of diquarks is quite similar with that of mesons with the corresponding quantum numbers. In particular, the scalar diquark $(\bar{\psi}_c i\gamma_5 \psi)$, which corresponds to the pion $(\bar{\psi} i\gamma_5 \psi)$, shows a strong quark-quark correlation, whereas the axial-vector diquark $(\bar{\psi}_c \gamma_\mu \psi)$, which corresponds to the rho meson $(\bar{\psi} \gamma_\mu \psi)$, is a weakly bound quark-quark state. If the coupling constants satisfy the condition $G_S^M = G_S^D$ and $G_V^M = G_V^D$, the diquark mass is the same as the corresponding meson mass, which is so-called the Pauli-Gürsey symmetry between mesons and diquarks[14, 26, 27]. Note that the strong diquark correlation in the scalar channel causes the large enhancement of the $\Delta I = 1/2$ transition matrix elements of the hyperon non- leptonic weak decays[13, 14].

The nucleon properties such as the mass and the wave function within the NJL model should be obtained by solving the relativistic three body problems, and such an effort is being made with the relativistic Faddeev method[28]. It seems, however, necessary to incorporate confinement for a successful description of baryons, which is absent in the NJL model. Therefore, we simply assume the diquark-quark model for the nucleon, and consider the case

of diquark-quark vertex being scalar[20];

$$\Gamma_{Dq}(p^2) \propto \mathbf{1} \cdot \phi(p^2) \quad (6)$$

where $\mathbf{1}$ is the unit matrix in the Dirac space and $\phi(p^2)$ is a regularization dependent function to be specified later. The diquark properties are obtained by solving the NJL model, which tells us the information of the quark-quark correlations.

4. Calculations of Hadronic Tensor

First, we evaluate contributions shown in Fig.1(a), where a quark is struck out by the virtual photon with the residual diquark being a spectator. This part can be calculated following the work of Meyer and Mulders[20]. We use the impulse approximation, and thus the hadronic tensor is represented by an incoherent sum of various processes. We define the constituent quark mass m and the diquark mass m_D inside the nucleon, though the diquark and the quark are not the eigenstates of QCD. Their values are obtained within the NJL model. The calculation of the hadronic tensor in the Bjorken limit yields[20],

$$\begin{aligned} q^D(x) &= \int \frac{d^4 p}{(2\pi)^4} \frac{\phi^2}{(p^2 - m^2)^2} 2\pi \delta(p_2^2 - m_D^2) \theta(p_2^0) \\ &\quad \times \frac{1}{2M\nu} \text{Tr}[(\not{p} + m)\gamma^+(\not{p} + m)(\not{P} + m)] \\ &= \int_{p_E^2 \text{min}}^{\infty} \frac{dp_E^2}{8\pi^2} \frac{\phi^2(p_E^2)}{(p_E^2 + m^2)^2} [x(M^2 + 2mM - m_D^2) + m^2 + (1-x)p_E^2] \end{aligned} \quad (7)$$

where

$$p_{E\text{min}}^2 = \frac{x}{1-x} m_D^2 - xM^2,$$

and M is the nucleon mass. Here, P is the proton momentum, and p and p_2 are momenta of the struck quark and the spectator diquark, respectively.

As for the diquark process shown in Fig.1(b), we fold the quark distributions in diquarks with the diquark distributions in the nucleon. We use the NJL model for the calculation of the quark distributions in the diquarks. Note that these contributions to the structure

functions scale. The approximation of the convolution method may be good for the scalar diquark process, since the scalar diquark is a small object due to its strong correlation. In fact, the NJL model calculation gives a small radius $\leq 0.4\text{fm}$. Phenomenological estimates of the scalar diquark radius also provides small value[5, 10]. But the size of the axial-vector diquark is comparable with that of the nucleon, thus the convolution is not suitable for the calculation of the axial-vector diquark process. Assuming the quark-diquark vertex to be scalar as mentioned above, we obtain the diquark term as the convolution integral[22];

$$Q_D^i(x) = \int_x^1 dx/y F_{D/N}(y) D_{Di}(x/y) \quad (8)$$

$F_{D/N}(y)$ is a probability to find a diquark in the nucleon with the light-cone momentum fraction y . This part is evaluated in terms of the scalar vertex (6);

$$\begin{aligned} F_{D/N}(y) &= y \int \frac{d^4 k}{(2\pi)^4} \phi^2(k^2) \frac{2[M^2 + mM - P \cdot k]}{(k^2 - m_D^2)^2} \\ &\quad \times 2\pi\delta(k_2^2 - m^2)\delta(y - \frac{k^+}{M})\theta(k^+)\theta(M - k^+) \\ &= y \int_{t_{\min}} \frac{dt}{16\pi^2} \phi(t)^2 \frac{[(m_D + M)^2 + t]}{(t + m_D^2)^2}, \end{aligned} \quad (9)$$

where

$$t_{\min} = \frac{y}{1-y}m^2 - yM^2.$$

Here, the diquark carries the momentum q and the residual quark q_2 . $D_{Di}(x)$ is the quark distribution of the leading twist diquark structure function. For the calculation of $D_{Di}(x)$, we use the same procedure as done in the meson case within the NJL model[29]. For example, the quark distributions in the scalar diquark is given by,

$$\begin{aligned} D_S(x) &\propto g_{Sqq}^2 \int d\mu_E^2 \left[\frac{1}{\mu_E^2 + m^2} + x \frac{m_D^2}{(\mu_E^2 + m^2)^2} \right] f(\mu_E^2) \\ &\quad \times \theta(m_D^2 x(1-x) - xm^2 + (1-x)\mu_E^2). \end{aligned} \quad (10)$$

g_{Sqq} is the diquark-quark-quark coupling constant obtained by the NJL model calculation. $f(\mu_E^2)$ is the regularization function. Note that the form of (10) is the same as the quark distribution of the pion obtained in ref. [29], since the diquark structure is the same as that of the corresponding meson in the NJL model due to the relation[26, 27];

$$CS_F^T(q)C^{-1} = S_F(-q)$$

where C is the charge conjugation operator and S_F the quark propagator. The structure function of the axial-vector diquark is also calculated in the similar manner[30]. Thus, we get the convolution of the axial-vector diquark term.

The integrals (7), (9), and (10) go to infinity due to the non-renormalizability of the NJL model. To avoid the divergence, we introduce the regularization function $f(p^2)$ in the Euclidean space. There exists an difficulty in the introduction of the standard NJL cutoff for DIS process[31, 32]. Here, we use the Fermi distribution type cut-off function, which is consistent to the usual sharp cut-off method except for large momentum.

$$f(t) = \frac{1}{1 + \exp[(t - \Lambda^2)/a]} = \phi^2(t) \quad (11)$$

Here, we use $\Lambda \sim 1 GeV$ and $a \sim 0.1 GeV^2$ to reproduce the meson properties. We examine also other plausible form like the exponential cut-off for completeness. We obtain similar quark distributions except for the shape around $x \sim 1$, which depends on the high momentum behavior of the cut-off scheme.

5. Results and Discussions

We present here the calculated result on the structure function. Concerning the NJL model parameters, we take the current quark mass $m_o = 5.5 MeV$ as a semi-empirical value, and $G_S^M \Lambda^2 = 2G_V^M \Lambda^2 = 22.2$, $\Lambda = 860 MeV$, $a = 0.15 GeV^2$ which are fixed by the pion properties. For the diquark part, we treat the diquark masses as free parameters, and study their dependence of the structure function. By the analysis of the N- Δ mass splitting in the one-gluon exchange picture, the scalar diquark mass m_S was assumed to be $575 MeV$ [33],

and the axial-vector diquark mass m_A to be 200MeV higher than the scalar diquark mass[19, 20]. Much larger scalar-vector diquark mass difference was obtained in the instanton liquid model[34] or other models[10, 26]. Here, we assume $m_A = 775\text{MeV}$, which is consistent to the above arguments and comparable with the vector meson mass like ρ . Then, we investigate the scalar diquark mass dependence of the results. The quark correlation affects the quark distributions through the diquark masses.

We first show the quark distributions of various processes at the low energy scale in Fig.2. These distributions represent their strength of the correlation. The quark distribution $q^S(x)$ (solid curve), where the scalar diquark is a spectator, has a sharp distribution peaked at $x \sim 0.5$, because of the weakness of the interaction between the scalar diquark and the third quark due to the strong binding of the diquark in the scalar channel. $q^V(x)$ (dashed curve) shows slightly a broader distribution. $q^S(x)$ and $q^V(x)$ are almost unchanged from the results of ref. [20]. In addition, we have calculated newly the contributions from diquark process (Fig.1(b)). The momentum of two quarks in the scalar diquark is, compared to $q^S(x)$, peaked at small x ; $x \sim 0.25$, as shown by dotted line. Using these distributions, we can obtain the momentum ratio carried by each quark. For the scalar channel, we find at $m_S = 575\text{MeV}$

$$\langle xq^S \rangle : \langle xQ_D^S \rangle \sim 2.2 : 1 ,$$

where $\langle xq \rangle = \int_0^1 dx x q(x)$. This means that the u-quark with the scalar diquark being a spectator carries the largest part of the proton momentum, and the remaining small part is carried by the u-d scalar diquark due to the strong correlation in the scalar channel. This result is consistent with the QCD sum rule[6, 7]. If the diquark correlation becomes weak, we find that this ratio is close to 1. For example, $\langle xq^S \rangle : \langle xQ_D^S \rangle \sim 1.3 : 1$ at $m_S = 775\text{MeV}$. In the case of axial-vector diquark process, we obtain

$$\langle xq^V \rangle : \langle xQ_D^V \rangle \sim 1.3 : 1 .$$

Thus, both two quarks in the axial-vector diquark ($Q_D^V(x)$: dash-dotted curve) and the third quark ($q_V(x)$) have almost the same amount of the proton momentum. This fact reflects the weak correlation of quarks in the axial-vector diquark channel. Comparing $Q_D^S(x)$ with $Q_D^V(x)$, the difference of both distributions is not so evident. Originally, the shapes of

distributions in the scalar and axial-vector diquarks are quite different, as π and ρ in the meson case[30]. However, such a difference is washed out after the convolution with the entire diquark motion in the proton.

We take the low energy model scale $Q_o^2 = 0.2\text{GeV}^2$, which is used in ref. [35]. At this scale, the running coupling constant is still small; $\alpha_s(Q_o^2)/\pi \sim 0.4$. Thus, the inclusion of the second order QCD corrections gives a small change for the Q^2 evolution from our result within 10%[35]. We use the first order Altarelli-Parisi equation[36] with the $\Lambda_{QCD} = 250\text{MeV}$, in order to compare our result with experiment. For the sea quark and the gluon parts, we simply assume that these distributions vanish at $Q^2 = Q_o^2$, and are generated by the QCD evolution process.

The proton and the neutron structure functions $F_2^p(x)$ and $F_2^n(x)$ thus obtained at $Q^2 = 15\text{GeV}^2$ are shown in Fig.3 with experimental data[1], where we use $m_A - m_S = 200\text{MeV}$. Our result shows a reasonable agreement with data for $x > 0.4$, and is somewhat different for small x value. One of the possible solutions for this disagreement is to take into account the sea quark degrees of freedom explicitly at the low energy scale. The inclusion of the $\bar{q} - 4q$ or $q - 3q\bar{q}$ intermediate state at the model scale may change the shape of $F_2(x)$ at small x as introduced in ref. [17]. Comparing our calculated results with the ones of the MIT bag model[16, 17] or the diquark spectator model[20], our structure functions are distributed over much wider range of the Bjorken x . This fact is the consequence of the strong diquark correlation. We also show in Fig.3 the proton structure function without the diquark scattering part (Fig.1(a) only), in which we use $Q_o^2 = 0.2\text{GeV}^2$. This result is essentially the same as that of the previous model calculation without the diquark process[16-20]. This structure function has a sharp peak around $x \sim 0.3$, and disagrees with experiment. In order to reproduce the absolute values and the peak position of the experimental data, one must take a smaller value for the model scale Q_o^2 . In fact, a much smaller value for the low energy scale is used in the previous calculations[17, 18, 20] so as to obtain a better agreement with experiment.

We would like to discuss the dependence of the structure function on the low energy scale

Q_o^2 . The nucleon structure functions are shown in Fig.4, with the choice of the low energy scale $Q_o^2 = 0.125\text{GeV}^2$. The running coupling constant α_s at this scale is about two times larger than that for $Q_o^2 = 0.2\text{GeV}^2$. As compared with the result in Fig.3, the calculated structure functions are in a good agreement with experiment, especially at low x . However, the use of the perturbative QCD becomes less reliable at such a low Q_o^2 .

We discuss how the flavor structure of the structure function depends on the diquark correlation. The ratio $F_2^n(x)/F_2^p(x)$ is shown in Fig.5. Our result is in good agreement with experiment[1, 2, 3], in the case $m_A - m_S = 200\text{MeV}$. This is due to the dominance of u-quark distributions, namely $q^S(x)$, at large x , which is caused by the asymmetric momentum distributions of quarks and diquarks. In the middle x range, $x \sim 0.4$, the resulting ratio is close to 2/3, since this part of distributions is dominated by the diquark parts, i.e. $Q_D^S(x)$ and $Q_D^V(x)$. We find that our calculated result is somewhat smaller than experiment for small x . The inclusion of sea quark at the low energy scale enhances this ratio in the small x region, and may resolve this discrepancy. We also show in Fig.5 the case $m_A - m_S = 0, 100, 275\text{MeV}$. If we take the same values for the scalar and the axial-vector diquark masses, the ratio is close to 2/3. We also show the difference $F_2^p(x) - F_2^n(x)$ in Fig.6. The peak position of our result is consistent with experiment, but the absolute value is rather large. This behavior was found in the previous calculations in terms of other models.

6. Conclusion

In conclusion, we have studied the flavor structure of quark distributions based on the phenomenological diquark model. This model reproduces the asymmetric momentum distributions in the nucleon obtained by the QCD sum rule. The neutron to proton structure function ratio $F_2^n(x)/F_2^p(x)$ shows a good agreement with the available DIS data. The agreement is lost as the diquark correlation becomes weak. Our result indicates that the quark correlation, especially in the scalar channel, is important to understand the DIS data, which is also crucial for the low energy hadron properties such as the $\Delta I = 1/2$ non-leptonic weak transition. Although we consider the twist-2 contributions of the structure function in this

paper, twist-4 pieces of them give us much information about the quark-quark correlation[37]. The diquark-like correlation may be important to study such higher twist effects. Work along this line is in progress.

References

- [1] J.J. Aubert *et al.*, European Muon Coll., Nucl. Phys. **B293** (1987) 740
- [2] P. Amaudruz *et al.*, New Muon Coll., Phys. Rev. Lett. **66** (1991) 2716; Nucl. Phys. B371 (1992) 3
- [3] A.C. Benvenuti *et al.*, BCDMS Coll., Phys. Lett. **B237** (1990) 599
- [4] A. Donnachie and P.V. Landshoff, Phys. Lett. **B95** (1980) 437
- [5] S. Ekelin and S. Fredriksson, Phys. Lett. **B162** (1985) 373
- [6] V.L. Chernyak and A.R. Zhitnitsky, Phys. Rep. **112** (1984) 173
- [7] Z. Dziembowski and J. Franklin, Phys. Rev. **D42** (1990) 905
- [8] For a review, P. Stoler, Phys. Rep. **226** (1993) 103
- [9] J. Bailly *et al.*, EHS-RCBC-Coll., Z. Phys. **C31** (1986) 367
- [10] *Diquarks*, ed. M. Anselmio and E. Predazzi (1988), World Scientific
- [11] M. Ida and R. Kobayashi, Prog. Theor. Phys. **36** (1966) 846
- [12] D.B. Lichtenberg, L.J. Tassie and P.J. Keleman, Phys. Rev. **167** (1968) 1535
- [13] B. Stech, Mod. Phys. Lett. A6 (1991) 3113; Phys. Rev. **D36** (1987) 975
H.G. Dosch, M. Jamin and B. Stech, Z. Phys. **C42** (1989) 167
- [14] K. Suzuki and H. Toki, TMU preprint (1993)
- [15] R.L. Jaffe and G.G. Ross, Phys. Lett. **B93** (1980) 313
- [16] C.J. Benesh and G.A. Miller, Phys. Rev. **D36** (1987) 1344
- [17] A.W. Schreiber, A.I. Signal and A.W. Thomas, Phys. Rev. **D44** (1991) 2653, and references therein.

[18] L.S. Celenza and C.M. Shakin, Phys. Rev. **C27** (1983) 1561
 C.J. Benesh and G.A. Miller, Phys. Lett. **B215** (1988) 381
 R.P. Bickerstaff and T. Londergan, Phys. Rev. **D42** (1990) 3621
 M.R. Bate and A.I. Signal, J. Phys. **G18** (1992) 1875
 M. Tarini, L. Conci and U. Moschella, Nucl. Phys. **A544** (1992) 731

[19] F.E. Close and A.W. Thomas, Phys. Lett. **B212** (1988) 227

[20] H. Meyer and P.J. Mulders, Nucl. Phys. **A528** (1991) 589

[21] J.D. Sullivan, Phys. Rev. **D5** (1972) 1732

[22] P.J. Mulders, A.W. Schreiber and H. Meyer, Nucl. Phys. **A549** (1992) 498, and references therein.

[23] K. Suzuki, to be published

[24] M.I. Pakovic, Phys. Rev. **D13** (1976) 2128
 M. Anselmino and E. Predazzi, Phys. Lett. **B254** (1991) 203

[25] Y. Nambu and G. Jona-Lasinio, Phys. Rev. **122** (1961) 345, *ibid* **124** (1961) 246

[26] U. Vogl and W. Weise, Prog. Part. Nucl. Phys. **27** (1991) 195, and references therein.

[27] K. Suzuki and H. Toki, Mod. Phys. Lett. **A7** (1992) 2867

[28] C.J. Burden, R.T. Cahill and J. Praschifka, Aust. J. Phys. **42** (1989) 147
 A. Buck, R. Alkofer and H. Reinhardt, Phys. Lett. **B286** (1992) 29
 N. Ishii, W. Bentz and K. Yazaki, Phys. Lett. **B301** (1993) 165

[29] T. Shigetani, K. Suzuki and H. Toki, Phys. Lett. **B308** (1993) 383

[30] T. Shigetani, K. Suzuki and H. Toki, TMU preprint (1993)

[31] C.L. Korpa and U.-G. Meissner, Phys. Rev. **D41** (1990) 1679

[32] M. Burkardt and B.J. Warr, Phys. Rev. **D45** (1992) 958

[33] J.H. Donoghue and K.S. Sateesh, Phys. Rev. **D38** (1988) 360

- [34] T. Schafer, E.V. Shuryak and J.J.M. Verbaarschot, preprint; SUNY-NTG-92/45
- [35] M. Glük, E. Reya and A. Vogt, Z. Phys. **C48** (1990) 471
- [36] G. Altarelli and G. Parisi, Nucl. Phys. **B126** (1977) 298
- [37] S. Choi, T. Hatsuda, Y. Koike and Su H. Lee, Phys. Lett. **B312** (1993) 351

Figure Caption

Fig. 1 : The forward scattering amplitude ("handbag diagram") of the nucleon. The thin solid line represent the quark, and the shaded line the diquark. The nucleon and the virtual photon are depicted by the thick solid and wavy lines. For details and notation, see text.

Fig. 2 : The quark distributions of the nucleon at the low energy scale $Q^2 = Q_o^2$ as a function of the Bjorken x . The solid and dashed curves denote the quark distributions obtained by the calculation of Fig.1(a) with the residual diquarks being scalar or axial-vector, respectively. The dotted and dash-dotted curves represent the distributions of the scalar and axial-vector diquark scattering processes (Fig.1(b)).

Fig. 3 : The proton and neutron structure functions at $Q^2 = 15GeV^2$. The solid curve represents $F_2^p(x)$, and the dashed curve $F_2^n(x)$. The proton structure function calculated without diquark scattering processes is depicted by the dotted curve. Here, we use the low energy model scale $Q_o^2 = 0.2GeV^2$. The experimental data are taken from the EMC experiment[1].

Fig. 4 : The proton and neutron structure functions at $Q^2 = 15GeV^2$. The notations are the same as those of Fig. 3. The low energy scale $Q_o^2 = 0.125GeV^2$ is used.

Fig. 5 : The ratio of the nucleon structure functions F_2^n/F_2^p at $Q^2 = 15GeV^2$ with $m_A - m_S = 0, 100, 200, 275MeV$ ($Q_o^2 = 0.2GeV^2$). The experimental data are taken from refs. [1-3].

Fig. 6 : The difference of the nucleon structure functions at $Q^2 = 15GeV^2$ with $m_A - m_S = 0, 100, 200, 275MeV$ ($Q_o^2 = 0.2GeV^2$). The experimental values with error bars are taken from the EMC and BCDMS experiments[1, 3].

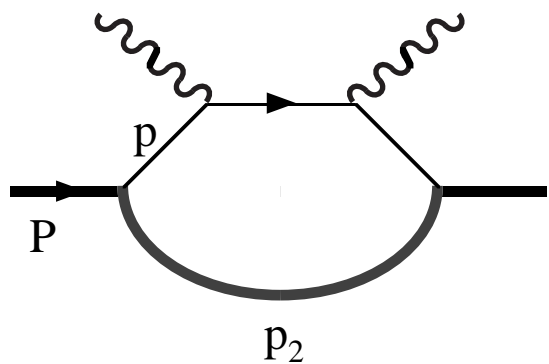


Fig. 1(a)

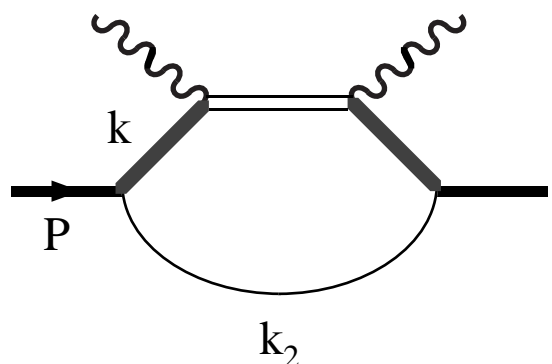
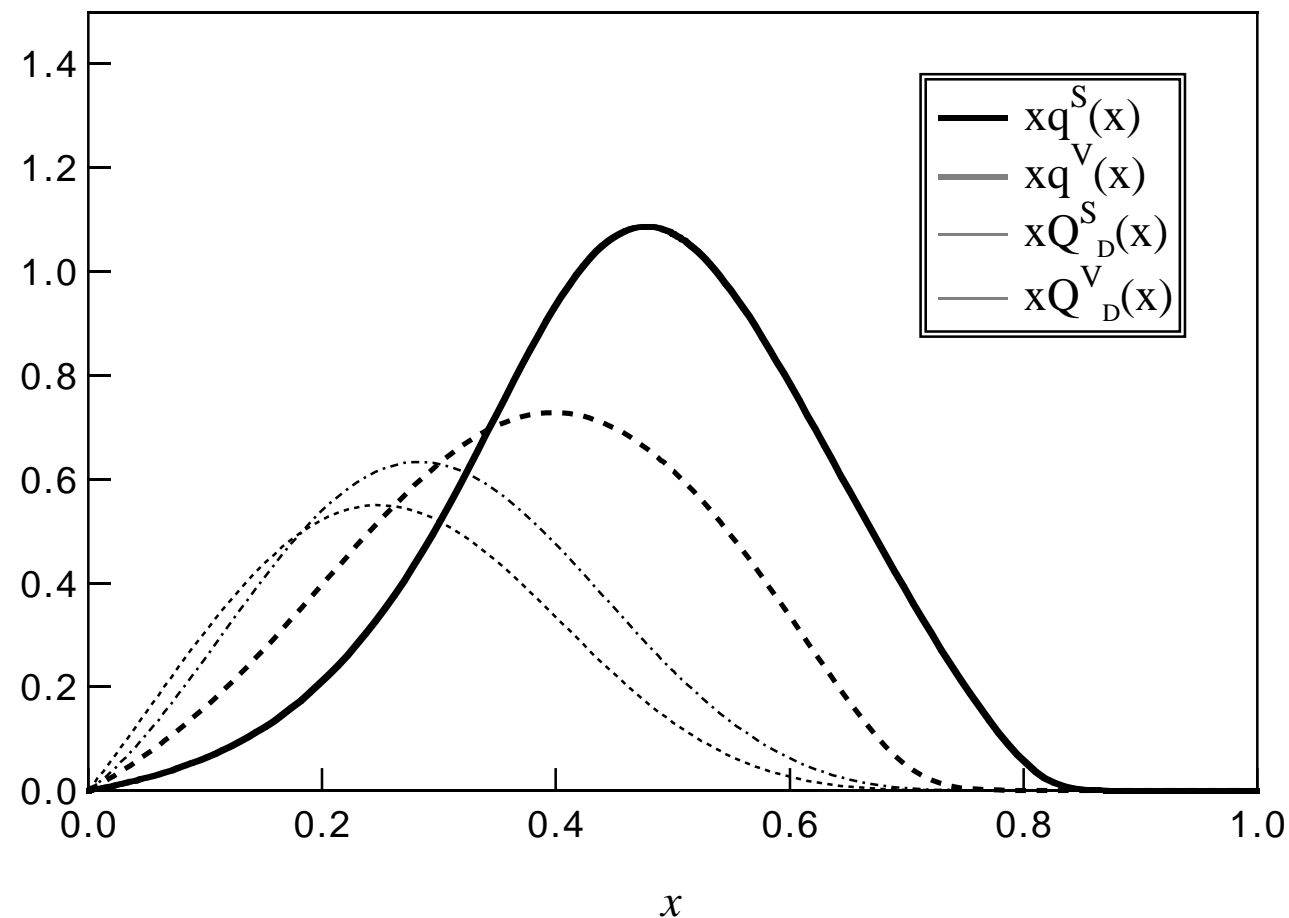


Fig. 1(b)

This figure "fig1-1.png" is available in "png" format from:

<http://arxiv.org/ps/hep-ph/9310266v1>

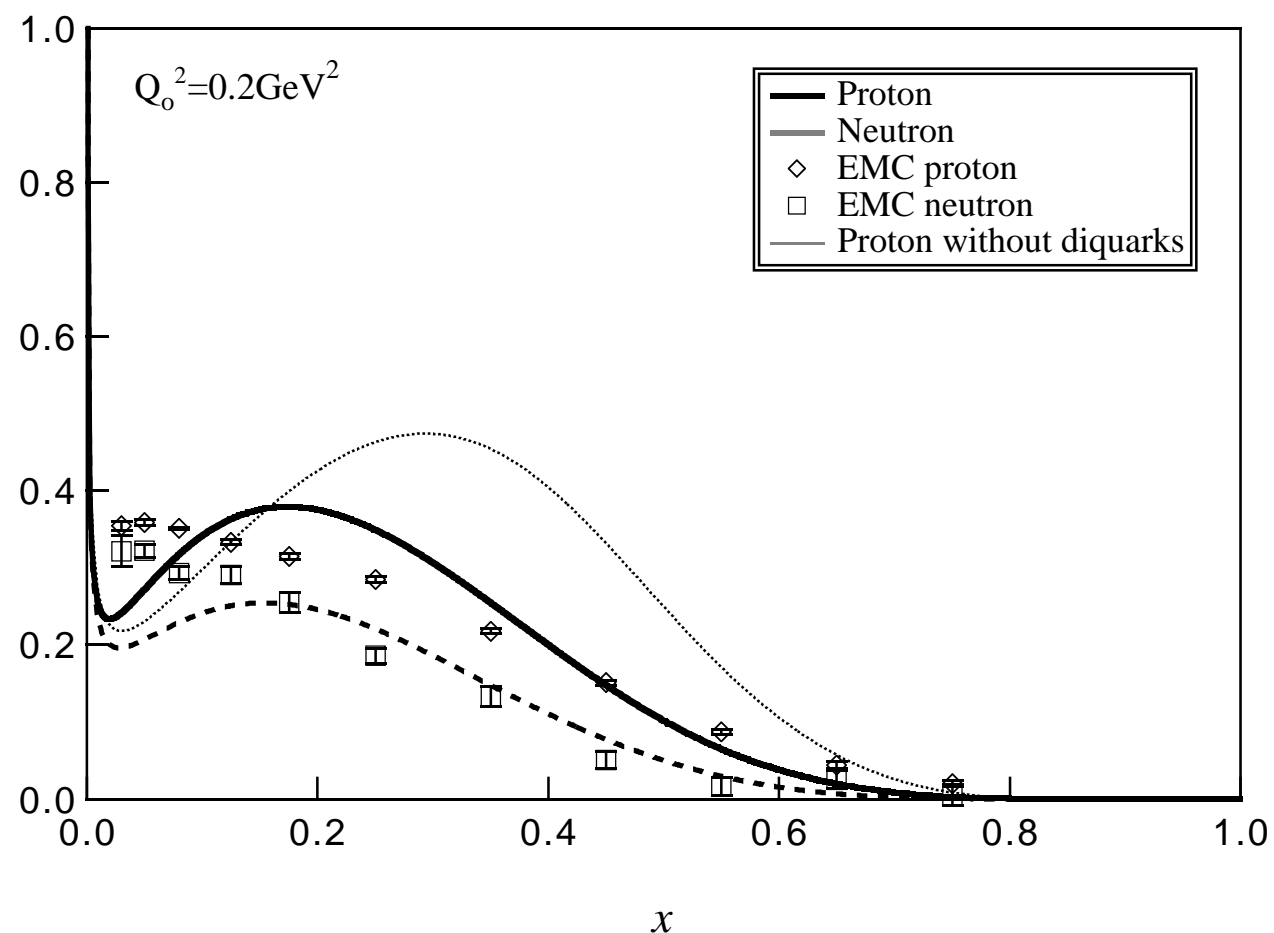
Fig. 2



This figure "fig1-2.png" is available in "png" format from:

<http://arxiv.org/ps/hep-ph/9310266v1>

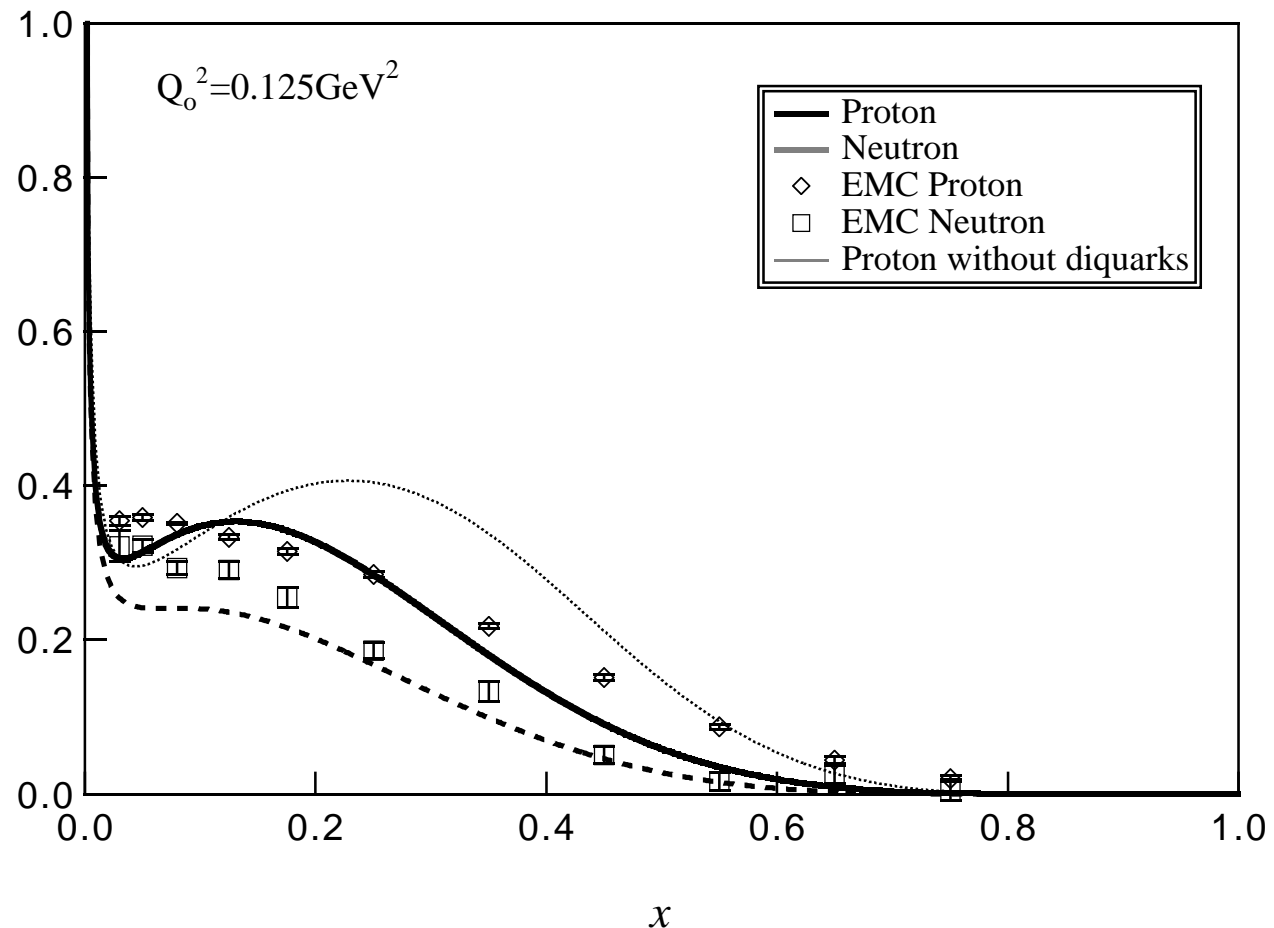
Fig. 3



This figure "fig1-3.png" is available in "png" format from:

<http://arxiv.org/ps/hep-ph/9310266v1>

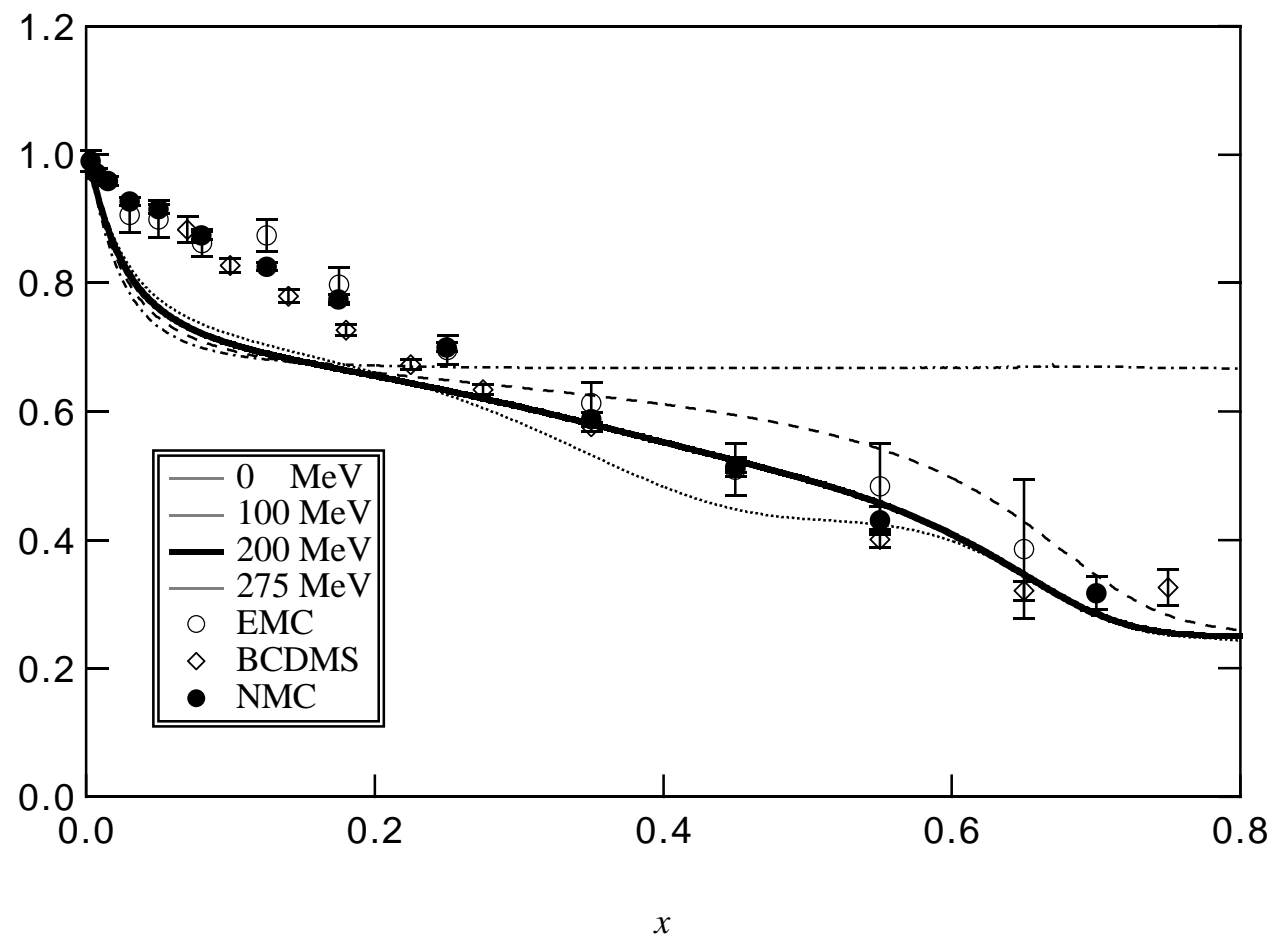
Fig. 4



This figure "fig1-4.png" is available in "png" format from:

<http://arxiv.org/ps/hep-ph/9310266v1>

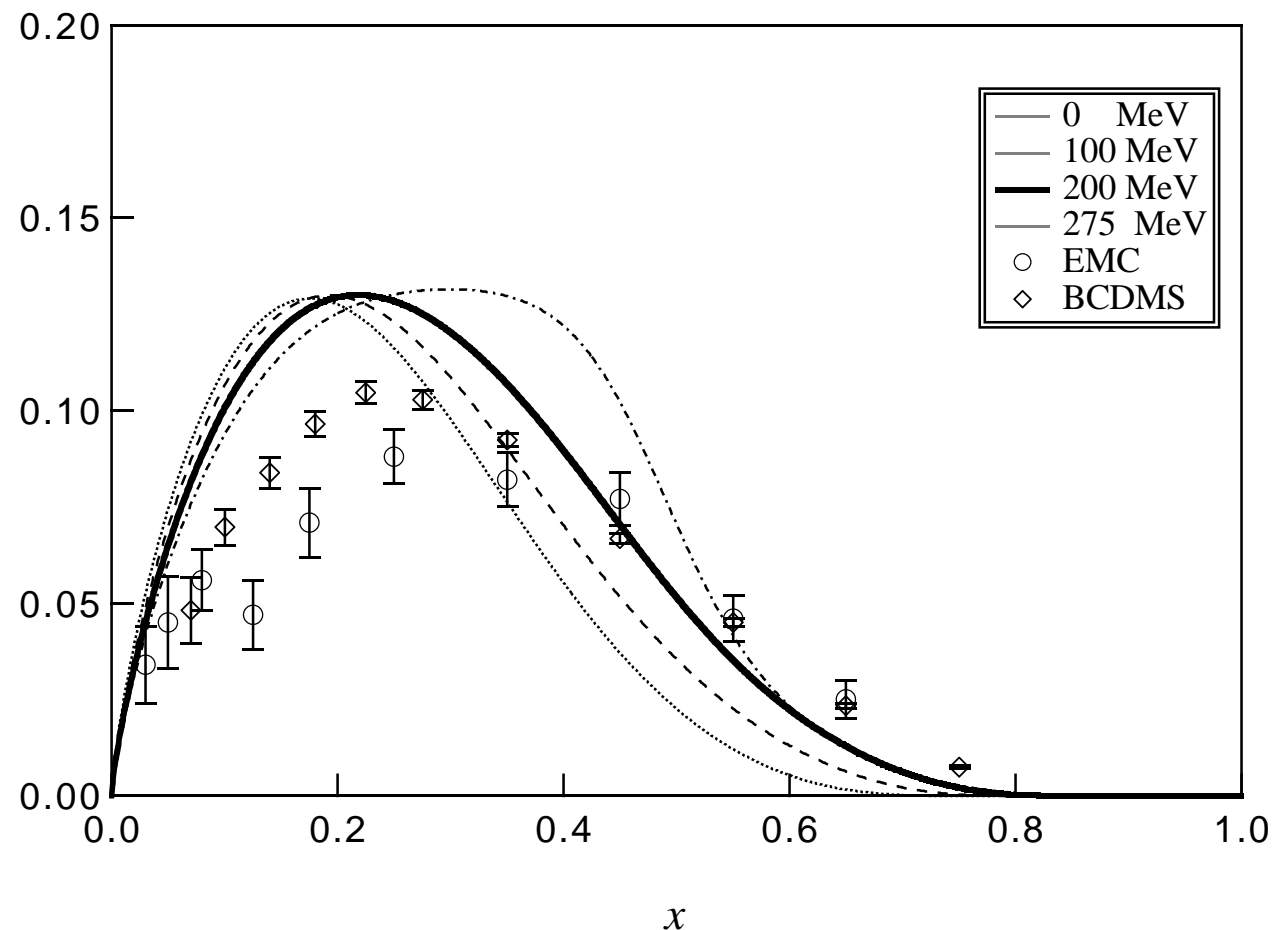
Fig. 5



This figure "fig1-5.png" is available in "png" format from:

<http://arxiv.org/ps/hep-ph/9310266v1>

Fig. 6



This figure "fig1-6.png" is available in "png" format from:

<http://arxiv.org/ps/hep-ph/9310266v1>